Journal of Advanced Research 61 (2024) 239–251

Contents lists available at ScienceDirect

Journal of Advanced Research

journal homepage: www.elsevier.com/locate/jare

CDK2-activated TRIM32 phosphorylation and nuclear translocation promotes radioresistance in triple-negative breast cancer

Jianming Tang [a,b,1,*], Jing Li [b,1], Jiayan Lian [c,1], Yumei Huang [d,1], Yaqing Zhang [e,1], Yanwei Lu [f], Guansheng Zhong [g], Yaqi Wang [b], Zhitao Zhang [b], Xin Bai [b], Min Fang [f], Luming Wu [h], Haofei Shen [h], Jingyuan Wu [h], Yiqing Wang [h,*], Lei Zhang [i,*], Haibo Zhang [f,*]

[a] Department of Radiation Oncology, The First Hospital of Lanzhou University, Lanzhou University, Lanzhou, Gansu 730000, PR China
[b] The First School of Clinical Medicine, Lanzhou University, Lanzhou, Gansu 730000, PR China
[c] Department of Pathology, The 7th Affiliated Hospital of Sun Yat-Sen University, Shenzhen 510275, Guandong, PR China
[d] Cancer Center, Department of Medical Oncology, Zhejiang Provincial People's Hospital (Affiliated People's Hospital), Hangzhou Medical College, Shangtang Road 158, Hangzhou, Zhejiang 310014, PR China
[e] Department of Obstetrics and Gynecology, Gansu Provincial Maternity and Child-care Hospital, Lanzhou, Gansu 730050, PR China
[f] Cancer Center, Department of Radiation Oncology, Zhejiang Provincial People's Hospital (Affiliated People's Hospital), Hangzhou Medical College, Hangzhou, Zhejiang 310014, PR China
[g] Department of Breast Surgery, The First Affiliated Hospital, College of Medicine, Zhejiang University, Hangzhou 310003, PR China
[h] Gansu International Scientific and Technological Cooperation Base of Reproductive Medicine Transformation Application, The First Hospital of Lanzhou University, Lanzhou University, Lanzhou, Gansu 730000, PR China
[i] Department of Radiation Oncology, Renji Hospital, School of Medicine, Shanghai Jiao Tong University, Shanghai 200127, PR China

HIGHLIGHTS

- Radiotherapy promotes the binding of CDK2 and TRIM32, thus leading to increased CDK2-dependent phosphorylation of TRIM32 at serines 328 and 339.
- Cis-trans isomerization of TRIM32 recruit PIN1, which resulting in importin α3 binding to TRIM32 and contributing to its nuclear translocation.
- Nuclear TRIM32 inhibits TC45-dephosphorylated STAT3, Leading to increased transcription of STAT3 and radioresistance in triple-negative breast cancer (TNBC).
- Regulating the CDK2/TRIM32/STAT3 pathway is a promising strategy for reducing radioresistance in TNBC, which is important for TNBC therapy.

GRAPHICAL ABSTRACT

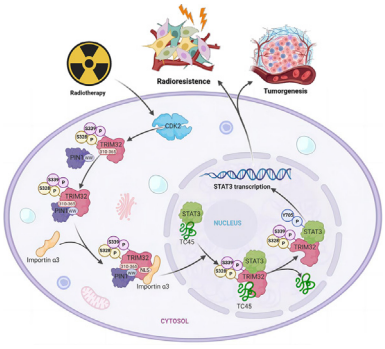

ARTICLE INFO

Article history:
Received 19 June 2023
Revised 4 September 2023

ABSTRACT

Introduction: Despite radiotherapy being one of the major treatments for triple-negative breast cancer (TNBC), new molecular targets for its treatment are still required due to radioresistance. CDK2 plays a

* Corresponding authors at: Department of Radiation Oncology, The First Hospital of Lanzhou University, Lanzhou University, Lanzhou, Gansu 730000, PR China (J. Tang). Gansu International Scientific and Technological Cooperation Base of Reproductive Medicine Transformation Application, The First Hospital of Lanzhou University, Lanzhou University, Lanzhou, Gansu 730000, PR China (Y. Wang). Department of Radiation Oncology, Renji Hospital, School of Medicine, Shanghai Jiao Tong University, Shanghai 200127, PR China (L. Zhang). Cancer Center, Department of Radiation Oncology, Zhejiang Provincial People's Hospital (Affiliated People's Hospital), Hangzhou Medical College, Hangzhou, Zhejiang 310014, PR China (H. Zhang).

E-mail addresses: ldyy_tangjm@lzu.edu.cn (J. Tang), ldyy_wangyq@lzu.edu.cn (Y. Wang), hrbmuzl@126.com (L. Zhang), zhbdoctor@163.com (H. Zhang).

[1] These authors contributed equally to this work.

https://doi.org/10.1016/j.jare.2023.09.011

Accepted 14 September 2023
Available online 19 September 2023

Keywords:
CDK2
TRIM32
Nuclear translocation
Radioresistance
Triple-negative breast cancer

critical role in TNBC. However, the mechanism by which CDK2 promotes TNBC radioresistance remains to be clearly elucidated.
Objectives: We aimed to elucidate the relationship between CDK2 and TRIM32 and the regulation mechanism in TNBC.
Methods: We performed immunohistochemical staining to detect nuclear TRIM32, CDK2 and STAT3 on TNBC tissues. Western blot assays and PCR were used to detect the protein and mRNA level changes. CRISPR/Cas9 used to knock out CDK2. shRNA-knockdown and transfection assays also used to knock out target genes. GST pull-down analysis, immunoprecipitation (IP) assay and in vitro isomerization analysis also used. Tumorigenesis studies also used to verify the results in vitro.
Results: Herein, tripartite motif-containing protein 32 (TRIM32) is revealed as a substrate of CDK2. Radiotherapy promotes the binding of CDK2 and TRIM32, thus leading to increased CDK2-dependent phosphorylation of TRIM32 at serines 328 and 339. This causes the recruitment of PIN1, involved in cis–trans isomerization of TRIM32, resulting in importin α3 binding to TRIM32 and contributing to its nuclear translocation. Nuclear TRIM32 inhibits TC45-dephosphorylated STAT3, Leading to increased transcription of STAT3 and radioresistance in TNBC. These results were validated by clinical prognosis confirmed by the correlative expressions of the critical components of the CDK2/TRIM32/STAT3 signaling pathway.
Conclusions: Our findings demonstrate that regulating the CDK2/TRIM32/STAT3 pathway is a promising strategy for reducing radioresistance in TNBC.

Introduction

TNBC is the deadliest subtype of breast cancer and has high heterogeneity and aggressiveness [1]. Despite recent postoperative radiotherapy advances, the median overall survival (OS) of TNBC patients is 10.2 months, highlighting the urgent need for new molecular targets to combat radioresistance, contributing to poor outcomes and unsuccessful therapy [2–3]. Recent findings have shown that protein kinase disorders commonly occur in various cancers including TNBC, and play critical roles in malignant biological behaviors [4–5]. Furthermore, protein kinases were demonstrated to be involved in cancer radioresistance [6–7]. However, protein kinase-targeted therapies improving radioresistance for TNBC remain explored.

Cell cycle is one of the main processes of cell proliferation and is regulated by the cyclin-dependent kinase (CDKs) family. Cyclin-dependent kinase 2 (CDK2) is a member of CDKs, activated by binding partner cyclins [8]. CDK2 regulates the cell cycle phase and plays a vital role in many biological processes, such as signal transduction, DNA damage, intracellular transport, protein degradation, DNA/RNA translation and metabolism [9–10]. CDK2 regulates the cell cycle from the late G1-phase and throughout S-phase by interacting with and phosphorylating proteins in cell signaling pathways [11]. Emerging evidence reveals the presence of CDK2 dysregulation in many human cancers, which is related to cancer cell proliferation [12]. CDKs were reported to regulate breast cancer proliferation and therapy resistance, especially CDK2 [13]. TNBC was reported to have a more aggressive phenotype than other subtypes. CDK2 was reported to closely associated with the OS of TNBC patients by regulating damage in DNA replication and repair pathways of TNBC cells [14], which shows its therapeutic potential for TNBC. The combination therapy of tamoxifen and CDK2 inhibitor was shown to effectively suppress TNBC growth and improve the survival in vivo [15]. However, it remains clear about how CDK2 regulates radioresistance in TNBC.

TRIM32, a protein of the RING-type E3 ubiquitin ligase family [16–18], is involved in cancer initiation and progression [19–21]. TRIM32 was proven to promote the gastric cancer cells growth by activated AKT pathway and glucose transportation [22]. Our previous study revealed through inhibiting TC45-dephosphorylated STAT3, TRIM32 effectively enhance TNBC radioresistance [23]. In this study, we first present evidence that TRIM32 acts as a substrate of CDK2 in radiotherapy-driven TNBC. Radiotherapy promoted CDK2-phosphorylated TRIM32 at serine 328 and 339, leading to nuclear translocation of TRIM32 via cis–trans isomerization, which involved the PIN1/importin α3 axis. Nuclear TRIM32 then inhibited TC45-dephosphorylated STAT3, Leading to increased transcription of STAT3 and radioresistance in TNBC. In this study, the novel radioresistance mechanism of CDK2-TRIM32-STAT3 was demonstrated in TNBC and might be potential radiotherapy targets.

Materials and Methods

Cell lines

BT549 and MDA-MB-231 cells were obtained from Shanghai Institute for Biological Sciences (Shanghai, China). Cells were maintained in Roswell Park Memorial Institute-1640 (RPMI-1640) supplemented with 100 U/ml penicillin–streptomycin and 10% fetal bovine serum (FBS). The cells were cultured in the humidified incubator at 37 ℃ and 5% carbon dioxide. STR DNA fingerprinting was performed on all the cell lines by Shanghai Biowing Applied Biotechnology Co., Ltd. The Lookout Mycoplasma PCR Detection Kit (Sigma-Aldrich) was detected for Mycoplasma contamination. The ionizing radiation (IR) dosage is 4 Gy. The radiation used a 6 MV X-ray linear accelerator at a dose rate of 200 Mu/min (Primus, Siemens AG, Erlangen, Germany).

Patient specimens

TNBC human tissue was collected at Zhejiang Provincial People's Hospital (Hangzhou, China). The number of samples collected is 116. The Research Ethics Board of the Zhejiang Provincial People's Hospital approved the study (QT2022272). All participants in the study received written informed consent, and none of the patients had received radiotherapy or chemotherapy prior to surgery.

shRNA-knockdown, sgRNA-knockout, and transfection assays

shRNA knockdown, sgRNA knockout, and transfection tests were carried out as described earlier [28]. The CDK1, 2, 4 and 5 sgRNA sequences have been designed by MIT on-line (https://

crispr.mit.edu). The shRNA sequence was acquired from Shanghai Bioegene Corporation (Shanghai, China).

Plasmids

TRIM32, CDK2, importin α (α1, α3, α4, α5, α6, and α7), PIN1, STAT3, and TC45 DNAs (cDNAs) or mutants were purchased from Shanghai Bioegene Co., Ltd. (Shanghai, China). Subsequently, they were sequenced and subcloned to either pLVX-Puro or pcDNA3.3 (Clontech). The wild type cDNA was cloned into the pGEX-4 T-1 vector to construct GST-CDK2.

Antibodies

Antibodies for GAPDH (1:5000 for WB, ab8245), TRIM32 (1:500 for WB, 1:50 for IP, ab96612), CDK2 (1:1000 for WB, A0094), p-CDK2 (T14) (1:1000 for WB, 1:50 for IHC, #2351–1), GST (1:1000 for WB, sc-138), PIN1 (1:1000 for WB, ab12107), Flag M2 (1:1000 for WB, 1:200 for IP, F3165), HA (1:1000 for WB, 1:200 for IP, #66006–1-Ig), CDK1 (1:1000 for WB, #19532–1-AP), CDK4 (1:2000 for WB, #11026–1-AP), CDK5 (1:1000 for WB, sc-249), Importin α3 (1:1000 for WB, IMG-3569), Lamin B1 (1:5000 for WB, AF5161), p-STAT3 (Y705) (1:1000 for WB, 1:50 for IHC, D3A7), STAT3 (1:1000 for WB, ab226942), TC45 (1:500 for WB, D7T7D), V5 (1:1000 for WB, ab107244), His (1:1000 for WB, #2365), phosphoserine/threonine antibody (1:1000 for WB, #612548), and β-Tubulin (1:5000 for WB, 3G6) were used. In a pay-for-service vendor, A rabbit polyclonal anti-phospho-TRIM32^{S339} antibody was raised by immunizing animals with a synthetic phospho-peptide corresponding to residues surrounding S339 of human TRIM32. Another rabbit polyclonal anti-phospho-TRIM32S^{328} antibody was also raised by immunizing animals.

IP and WB assays

IP and WB analyses were performed as previously described [63]. Cells were lysed and then incubated in IP lysis buffer (pH 7.5, 20 mM Tris-HCl, 150 mM NaCl, 2 mM Na3VO4, 1% Triton X-100, 1 mM EDTA, 5 mM NaF), supplemented with protease inhibitor cocktail) at 4 °C for 30 min. The lysates were separated by centrifuging. Specific antibodies and protein A/G magnetic beads (Invitrogen) were used for immunoprecipitation of cell lysates with equal amounts. Then, WB assay was used. The statistical charts of western blot were shown in Supplementary Fig. 8-9.

Purification of recombinant proteins and GST pull-down assay

Purification of recombinant proteins was performed as previously described[64]. Recombinant (His)6-tagged TRIM32 were lysed, sonicated, and centrifuged. Then, a Ni + -NTA column was used to purify the supernatants. pGEX-4 T-1-CDK2 was transformed into Escherichia coli BL21 and purified using glutathione beads in accordance with manufacturer's protocols. The GST pull down test was performed for 30 min using incubated purified GST-CDK2 proteins and the MDA-MB-231 cell extracts. Then, the Ni beads were washed.

Clonogenic cell survival assay

A suitable number of log-phase cells were plated in a six-well plate overnight and were expose in the X-rays at different dose (0, 2, 4, 6, 8 Gy). After irradiation, all plates were stored at 37 °C for 14 days in the cell incubator to allow colony formation. After 14 days of culture, cell clones were fixed with 4% formaldehyde, which were then treated with crystal violet solution for 30 min. Colonies with more than 50 cells were evaluated.

In vitro kinase assay

HA-CDK2 plasmids and purified recombinant (His)6-TRIM32 WT or S328A or S339A proteins were transfected into cells. Co-immunoprecipitation of cell lysates was performed, and SDS-PAGE was used to analyze the reaction.

In vitro isomerization analysis

In vitro isomerization analysis was performed as previously described [54]. The peptide was incubated for 2 min with α-chymotrypsin at 0 °C to completely hydrolyze the trans isomer at 4-nitroanilide bond. The pure cis peptides were re-equilibrated, and the isomerisation was carried out. At the indicated time, an aliquot was taken, and 4-nitroaniline was measured at 405 nm. The content of *cis*-peptide showed the isomerization rate.

RNA isolation and qRT-PCR

Total RNA was isolated from cells utilizing TRIzol (Takara, Dalian, China) and transcribed into cDNA using Reverse Transcription Kit (Takara, Dalian, China). The SYBR Green Master PCR mixture (Clontech, USA) was then used to perform qPCR. The primers are as described below. For control GAPDH amplification: 5′-GGAGCGAGATCCCTCCAAAAT-3′ and 5′-GGCTGTTGTCATACTTCT CATGG-3′; for control TRIM32 amplification: 5′-CCGGGAAGTGCTA GAATGCC-3′ and 5′-CAG CGGACACCATTGATGCT-3′; for control SOCS3 amplification: 5′-CCTGCGCCTCA AGACCTTC-3′ and 5′-GTC ACTGCGCTCCAGTAGAA-3′; for control c-FOS amplification: 5′-CC GGGGATAGCCTCTCTTACT-3′ and 5′-CCAGGTCCGTGCAGA AGTC-3′.

Immunohistochemical (IHC) staining

The paraffin-embedded TNBC specimens were stained with TRIM32(1:100), p-CDK2^{T14} (1:50), p-TRIM32^{S339} (1:100), and p-STAT3^{Y705} (1:50) antibodies. The number of samples is 116 paraffin-embedded TNBC specimens. Negative control slides without primary antibodies were used as negative controls. Each specimen was scored according to the staining intensity (3 = strong staining, 2 = moderate staining, 1 = weak staining, 0 = no staining) and the proportion of positive cells (4 = 75–100%, 3 = 50–75%, 2 = 25–50%, 1 = 1–25%,0 = 0%). The total score = the staining score + the proportion score. Low expression tumors were defined as scores ranging from 0 to 2, whereas high expression tumors were defined as scores ranging from 3 to 7. Two individuals blinded to the clinical parameters was used in the tissue score calculation.

Rna-seq and differentially expressed gene analysis

Total RNA was extracted and purified in accordance with the manufacturer's specifications using Qiagen RNeasy Mini Kit (Valencia, CA, USA). The RNA quality was assessed prior to sequencing using the Agilent 2100 bioanalyzer. Poly (A) + RNA libraries were prepared in accordance with Illumina. The library was sequenced on the Illumina HiSeqX Ten platform. Differential expression was detected by fold change filtering (FOLD-CHANGE $\geq$ 2.0; P $\leq$ 0.05). KEGG pathway analysis was performed on the differentially expressed genes using DAVID software (https:// david.ncifcrf.gov/). The P values for KEGG pathways were calculated by Fisher's exact or chi-square test with FDR. For the selection of significant items, the threshold value was P < 0.05 and the FDR

was < 0.25. RNA data are available at the Gene Expression Omnibus under the accession GEO ID: GSE210030.

Tumorigenesis studies

4–5 weeks-old female athymic nude mice were purchased from Slaccas (Shanghai). The mice were divided into 5 groups at random, and 5×10^6 MDA-MB-231 cells were subcutaneously injected into each mouse. Tumor volumes were calculated using the following equation: tumor volume (mm^3) = (length × width^2)/2. Tumor sizes and weights were measured and calculated every 2 or 3 days. Nude mice subcutaneously injected with MDA-MB-231 cells were treated with Roscovitine only (Intraperitoneal injection, daily, 50 mg/kg concentration of Roscovitine), irradiation (10 Gy) only, or Roscovitine combination with 4 Gy irradiation when the tumor volumes reached 150 mm3 (7 days after injection). We observe xenograft tumors for 10 days after treatment. The radiation used a 6 MV X-ray linear accelerator at a dose rate of 200 Mu/min (Primus, Siemens AG, Erlangen, Germany). The animal experiments were approved by the Zhejiang Provincial People's Hospital's Research Ethics Board (Approval no. A20220012).

Statistical analysis

Clonogenic survival test was performed by means of one way variance analysis. The significance of the data between groups was determined by the Student's *t*-test or the Newman-Keulspost-Test (ANOVA). The survival analysis was performed using the Kaplan-Meier approach. The P value of < 0.05 was considered to be statistically significant.

Ethics statement

All experiments involving animals and human patient were conducted according to the ethical policies and procedures approved by the Zhejiang Provincial People's Hospital's Research Ethics Board (Approval no. A20220012 for animal study and QT2022272 for human study).

Results

Radiotherapy-promoted CDK2 increases TRIM32 nuclear translocation

We first performed immunohistochemical (IHC) staining to detect nuclear TRIM32 on 8 paired TNBC tissues which was preradiotherapy and postradiotherapy. TRIM32 expression is higher in postradiotherapy group. TRIM32 expression increases in a dose-dependent manner post-IR treatment (Supplementary Fig. 7A-B). Besides, immunofluorescence staining also demonstrated that radiotherapy promoted TRIM32 nuclear translocation (Supplementary Fig. 7C). Interestingly, radiotherapy significantly induced TRIM32 nuclear translocation (Fig. 1A and B). Further study

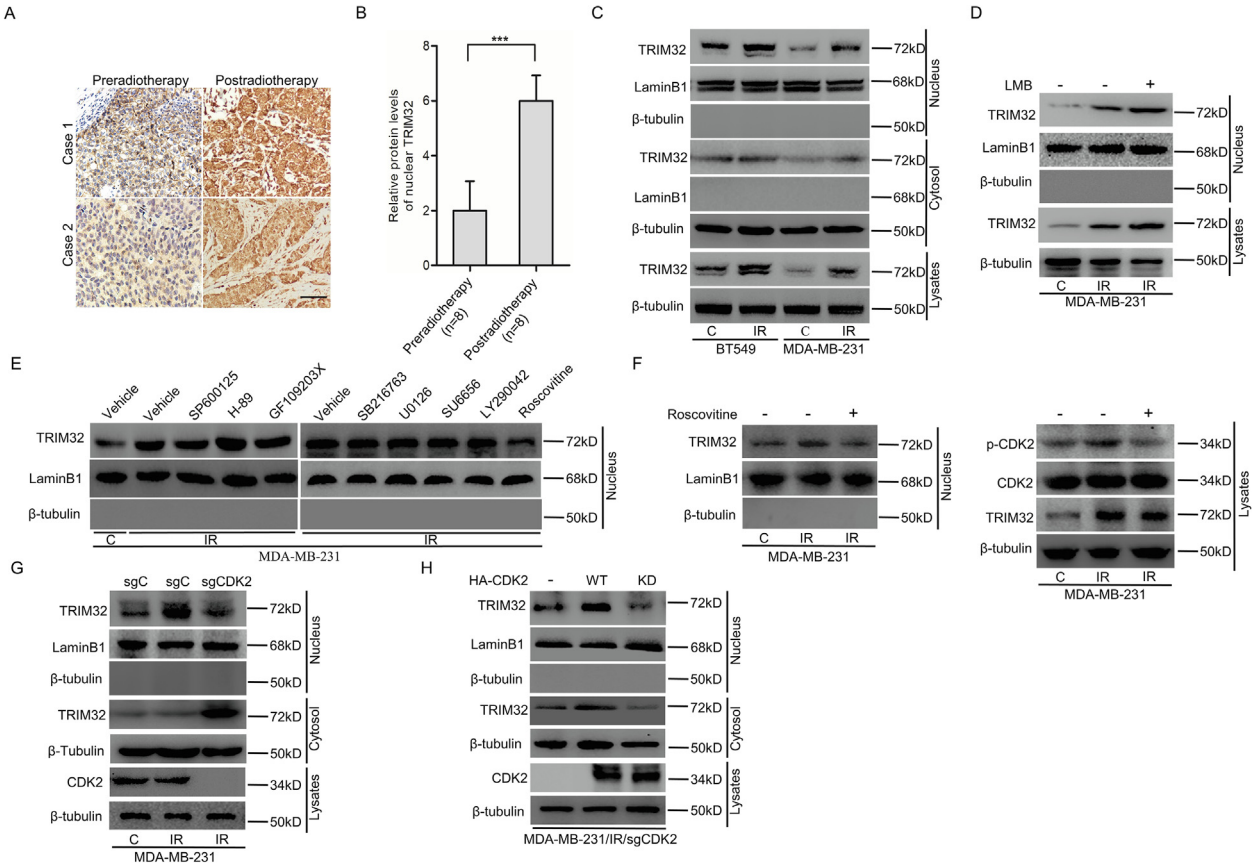

Fig. 1. Radiotherapy-promoted CDK2 increases TRIM32 nuclear translocation. A, IHC staining of TRIM32 protein levels in preradiotherapy and postradiotherapy specimens of TNBC. Scale bars: 50 μm. **B**, Quantitative analysis of TRIM32 expression in **A**. **C**, Effects of irradiation on nuclear TRIM32 protein expression. **D**, WB analysis of radiotherapy-induced TRIM32 nuclear translocation. Nuclear fractions were obtained from MDA-MB-231 cells. Nuclear lamin B1 and cytoplasmic β-tubulin were used as controls. **E**, Effects of kinase inhibitors on nuclear translocation of TRIM32. MDA-MB-231/irradiation cells were treated with SP600125 (25 μM), H-89 (30 μM), GF109203X (15 μM), SB216763 (10 μM), U0126 (25 μM), SU6656 (10 μM), LY290042 (30 μM) or Roscovitine (25 μM). F. **F**, Representative images of radiotherapy- induced TRIM32 nuclear translocation by WB analysis. **G**, Effect of CDK2 knockout on TRIM32 nuclear localization in MDA-MB-231/irradiation cells. **H**, WB analysis of HA-CDK2 WT or kinase-dead (KD) mutant on nuclear translocation of TRIM32 in MDA-MB-231/irradiation/sgCDK2 cells. Data are representative of three independent experiments with similar results.

demonstrated that TRIM32 nuclear translocation occurred in TNBC BT549 and MDA-MB-231 cells treated with irradiation (Fig. 1C). As shown in Fig. 1D, a leptomycin B (LMB), nuclear export inhibitor, retained radiotherapy- induced TRIM32 nuclear localization. These data suggest that radiotherapy inducement increases the nuclear translocation of TRIM32.

In order to discover which kinases are needed for the nuclear localization of TRIM32, MDA-MB-231/irradiation cells were treated with MEK inhibitor (U0126), c-Jun inhibitor (SP600125), Src inhibitor (SU6656), PKA inhibitor (H-89), GSK-3 inhibitor (SB216763), PKC inhibitor (GF109203X), PI3K inhibitor (LY290042), or CDK2 inhibitor (Roscovitine), respectively. As shown in Fig. 1E, only Roscovitine significantly impaired radiotherapy-induced TRIM32 nuclear translocation compared with the control groups. Western blot (WB) assays confirmed similar results (Fig. 1F).

Next, we investigated the influence of CDK2 on the nuclear accumulation of TRIM32. MDA-MB-231/irradiation cells were treated with the CRISPR/Cas9 to knock out CDK2. As shown in Fig. 1G, CDK2 knockout significantly abrogated radiotherapy- induced nuclear translocation of TRIM32. Furthermore, CDK2 wild-type (WT) and kinase-dead (KD) mutant vectors were constructed [24]. The results in Fig. 1H shows re-expression of CDK2 WT rescued TRIM32 nuclear translocation in MDA-MB-231/irradiation/sgCDK2 cells, but the same was not observed in the KD mutant. These results indicate that the activity of CDK2 kinase is essential for the nuclear translocation of TRIM32 induced by radiotherapy. Additionally, several relevant CDKs were knocked out in MDA-MB-231/irradiation cells, including CDK1, CDK2, CDK4, and CDK5, and found that only CDK2 knockout markedly impaired radiotherapy-induced nuclear translocation of TRIM32 (Supplementary Fig. 1).

CDK2 directly binds to and phosphorylates TRIM32

To reveal how CDK2 regulates radiotherapy-induced nuclear translocation of TRIM32, an immunoprecipitation (IP) assay in MDA-MB-231/irradiation and BT549/ irradiation cells was first performed, demonstrating that endogenous CDK2 interacted with TRIM32 (Fig. 2A). Radiotherapy increased CDK2 binding with TRIM32 in MDA-MB-231 and BT549 cells (Fig. 2B). Furthermore, purified recombinant CDK2 directly interacted with TRIM32 by GST pull-down analysis, which was markedly enhanced by radiotherapy (Fig. 2C). Next, truncated mutants D2 and D3 were constructed in MDA-MB-231/irradiation cells (Fig. 2D). Radiotherapy enhanced D2 but not D3 association with CDK2, revealing that the region of TRIM32 (amino acids 310–653) is necessary for its binding with CDK2 (Fig. 2E).

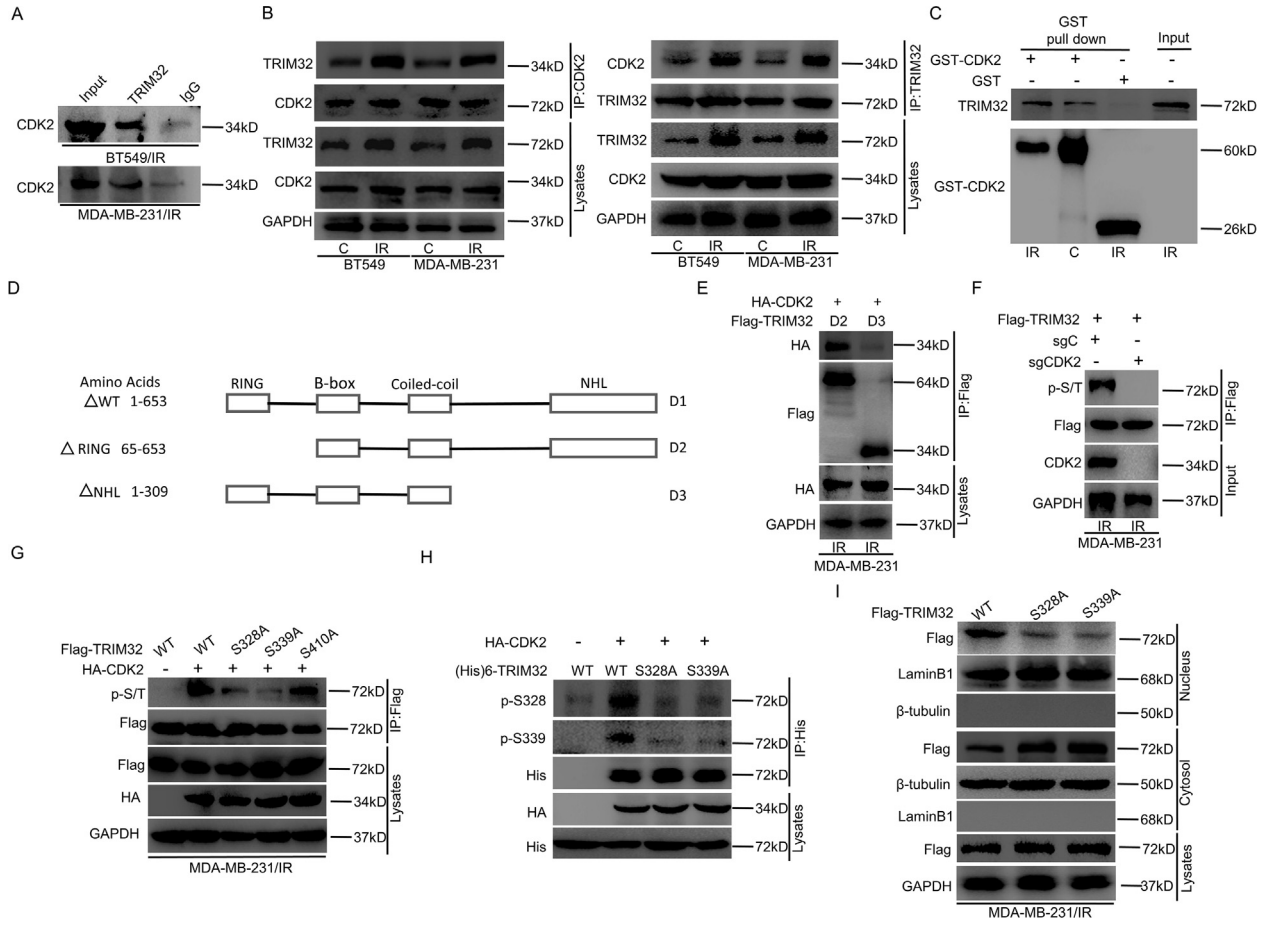

Fig. 2. CDK2 directly binds to and phosphorylates TRIM32. A, IP and WB assays for CDK2 associated with TRIM32 in MDA-MB-231/irradiation and BT549/ irradiation cells. **B**, IP and WB assays for CDK2 associated with TRIM32 in MDA-MB-231 and BT549 cells with or without radiotherapy. **C**, Effects of CDK2 associated with TRIM32 by in vitro GST pull-down analysis. **D**, Schematics of TRIM32 wild type and various truncated constructs. **E**, Effects of various truncated constructs of TRIM32 on the association between TRIM32 and STAT3 in MDA-MB-231/ irradiation cells. **F**, Effect of CDK2 knockout on p-Ser/Thr expression levels of TRIM32 in MDA-MB-231/irradiation cells. **G**, IP and WB assays for effects of TRIM32 WT, S328A, S339A, and S410A on TRIM32 phosphorylation in MDA-MB-231/irradiation cells transfected with HA-CDK2. **H**, in vitro kinase assay using purified 6 × His-TRIM32 WT or S328A, S339A and HA-CDK2. **I**, Localization of TRIM32 WT, S328A, and S339A mutant in MDA-MB-231/irradiation cells. Data are representative of three independent experiments with similar results.

To further demonstrate that TRIM32 is a substrate of CDK2, CDK2 was knocked out to assess its effect on TRIM32 phosphorylation. Fig. 2F showed that CDK2 knockout abrogated radiotherapy-induced phosphoserine/threonine (p-Ser/Thr) of TRIM32 in MDA-MB-231/irradiation cells. Next, in silico analysis was performed by the GPS 3.0 software (https://gps.biocuckoo.org). From the prediction, three possible phosphorylation sites of CDK2, S328, S339, and S410, were selected. The TRIM32 WT mutants S328A, S339A, and S410A were constructed to identify the role of the CDK2 phosphorylation sites. As shown in Fig. 2G, the S328A and S339A mutants markedly impaired radiotherapy-induced TRIM32 p-Ser/Thr in MDA-MB-231/ irradiation cells.

To further reveal CDK2 phosphorylation of TRIM32 at S328 and S339, we performed in vivo kinase analysis and confirmed that TRIM32 S328A and S339A, but not TRIM32 WT, had a significant effect on TRIM32 phosphorylation by CDK2 (Fig. 2H). These findings are in line with the results that CDK2 is associated with TRIM32 amino acids 310–653 residues, including residues S328 and S339 (Fig. 2E). Furthermore, the non-phosphorylatable S328A and S339A of TRIM32 mutation suppressed radiotherapy-induced nuclear translocation of TRIM32 (Fig. 2I), whereas the phosphor-mimic S328D and S339D of TRIM32 mutation induced in the nucleus upon radiotherapy activation (Supplementary Fig. 2). In conclusion, our results demonstrate that CDK2 binds to and phosphorylates TRIM32 directly at S328 and S339 sites, resulting in nuclear translocation of TRIM32.

S328/S339 sites of TRIM32 phosphorylation are required for recruiting PIN1

Pro-directed Ser/Thr phosphorylation was reported to be involved in protein conformational alteration and signaling pathway transduction [25]. A unique peptidyl-prolyl cis–trans isomerase, PIN1, mediates conformational alteration of p-Ser/Thr-Pro motifs [25–26]. To demonstrate how PIN1 mediates radiotherapy-induced TRIM32 nuclear translocation, IP assays were performed in MDA-MB-231/irradiation and BT549/irradiation cells, and explore the association between TRIM32 and PIN1. As shown in Fig. 3A, radiotherapy significantly enhanced PIN1 directly associated with TRIM32 in MDA-MB-231/irradiation and BT549/irradiation cells. Additionally, Roscovitine inhibited the interaction between TRIM32 and PIN1 (Fig. 3B). TRIM32 WT was correlated with PIN1 in MDA-MB-231/irradiation cells (Fig. 3C) but not S328A and S339A mutants. Moreover, the S328D and S339D mutants of TRIM32 showed stronger binding with PIN1

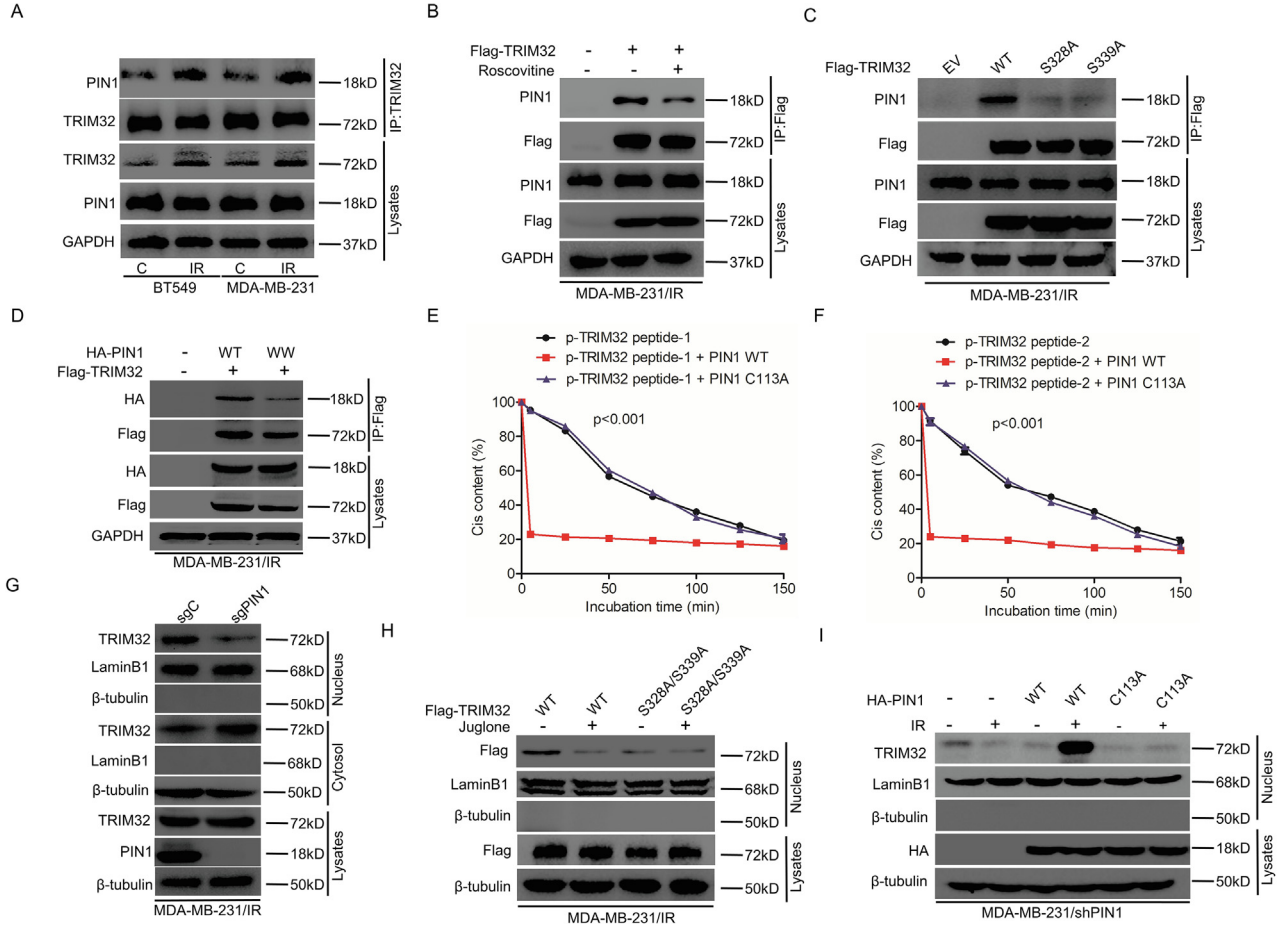

Fig. 3. S328/S339 sites of TRIM32 phosphorylation are required for recruiting PIN1. A, IP and WB assays for TRIM32 associated with PIN1 in MDA-MB-231 and BT549 cells with or without radiotherapy. **B**, IP and WB assays for TRIM32 binding with PIN1 in MDA-MB-231/irradiation cells. Cells were treated with or without Roscovitine (25 μM) for 1 h. **C**, Effects of TRIM32 WT, S328A, or S339A mutant on the association between TRIM32 and PIN1 in MDA-MB-231/irradiation cells. **D**, Effects of PIN1 WT or WW mutant on TRIM32 associated with PIN1. **E-F**, The phosphorylated S328/P329 (**E**) and S339/P349 (**F**) oligopeptides of TRIM32 are co-expressed with purified PIN1 WT or C113A mutant. Then cis–trans isomerization analysis was performed. Data were expressed as means ± SD. P values were calculated using one-way analysis of variance (ANOVA). **G,** WB assays for PIN1 knockout on nuclear localization of TRIM32 in MDA-MB-231/irradiation cells. **H**, MDA-MB-231/irradiation cells reconstituted with TRIM32 WT, S328A/S339A mutant were treated with or without PIN1 inhibitor Juglone (10 μM) for 4 h. **I**, Effects of re-expression of shRNA-resistant PIN1 WT or C113A mutant on nuclear translocation of TRIM32 with or without radiotherapy in MDA-MB-231/shPIN1 cells. Data are representative of three independent experiments with similar results.

than TRIM32 WT in MDA-MB-231/irradiation cells (Supplementary Fig. 3A). These results suggest that the S328/S339 sites of TRIM32 phosphorylation are necessary for TRIM32 associated with PIN1 in TNBC cells.

The PIN1 WW region interacts with p-Ser/Thr-Pro motifs [15]. To determine whether the PIN1 WW domain is required for TRIM32 binding to PIN1, Flag-TRIM32 was first overexpressed with HA-PIN1 WT or WW mutants (R14A, R17A, W11A, and W34A) in MDA-MB-231/irradiation cells. Fig. 3D indicated that only the PIN1 WT was associated with TRIM32, whereas the PIN1 WW mutants were not. Moreover, TRIM32 S328/P329 phosphorylation (p-TRIM32 peptide-1) and non-phosphorylation (TRIM32 peptide-1) peptides, TRIM32 S339/P340 phosphorylation (p-TRIM32 peptide-2) and non-phosphorylation (TRIM32 peptide-2) peptides were synthesized. As displayed in Fig. 3E and 3F, p-TRIM32 peptide-1 and p-TRIM32 peptide-2 showed more efficient isomerization by PIN1 WT compared with the catalytically inactive PIN1 C113A mutant. However, PIN1 WT did not isomerize TRIM32 peptide-1 and TRIM32 peptide-2 (Supplementary Fig. 3B and 3C).

Finally, PIN1 was knocked out in MDA-MB-231/irradiation cells to further elucidate the relevance of PIN1 in the nuclear translocation of TRIM32. Fig. 3G shows that PIN1 knockout markedly suppressed radiotherapy-induced TRIM32 nuclear translocation. Further study revealed that nuclear translocation of TRIM32 WT, but not S328A/S339A mutants, was greatly inhibited in MDA-MB-231/irradiation cells treated with PIN1 inhibitor Juglone (Fig. 3H). Reexpressing PIN1 WT but not C113A mutation, was able to rescue nuclear translocation of TRIM32 upon radiotherapy in MDA-MB-231/shPIN1 cells (Fig. 3I). These results indicate that the S328/S339 sites of TRIM32 phosphorylation are required for recruiting PIN1.

PIN1 induces phosphorylated TRIM32 at the S328 and S339 sites interacting with importin α3

The R68/69 residues of PIN1 play critical roles in its nuclear localization signal (NLS) [27–28]. HA-PIN1 WT or R68/69A mutant were overexpressed in MDA-MB-231/ shPIN1 cells to demonstrate the role of PIN1 NLS in the nuclear translocation of TRIM32. As shown in Fig. 4A, re-expression of PIN1 WT or R68/69A mutant rescued TRIM32 nuclear translocation upon radiotherapy in MDA-MB-231/shPIN1 cells, proven that PIN1′s NLS domain is not necessary for TRIM32 nuclear translocation. Therefore, we hypothesize that TRIM32 itself contains an NLS, and TRIM32′s NLS is exposed via its cis–trans isomerization regulated by PIN1. Next, in silico analyses were conducted with the NLStradamus software (https://www.moseslab.csb.utoronto.ca/NLStradamus/) [29]. From this analysis, one candidate NLS sequence was identified in TRIM32 at amino acid residues 145–168, RRRDFGEKLTRLRELMGELQRRKA (Fig. 4B). To identify whether TRIM32 nuclear translocation is dependent on TRIM32′ NLS, the TRIM32 WT and NLS mutant were constructed in MDA-MB-231/irradiation cells. In Fig. 4C, the TRIM32 NLS mutant suppressed radiotherapy-induced TRIM32 nuclear translocation, while the WT demonstrated no suppression.

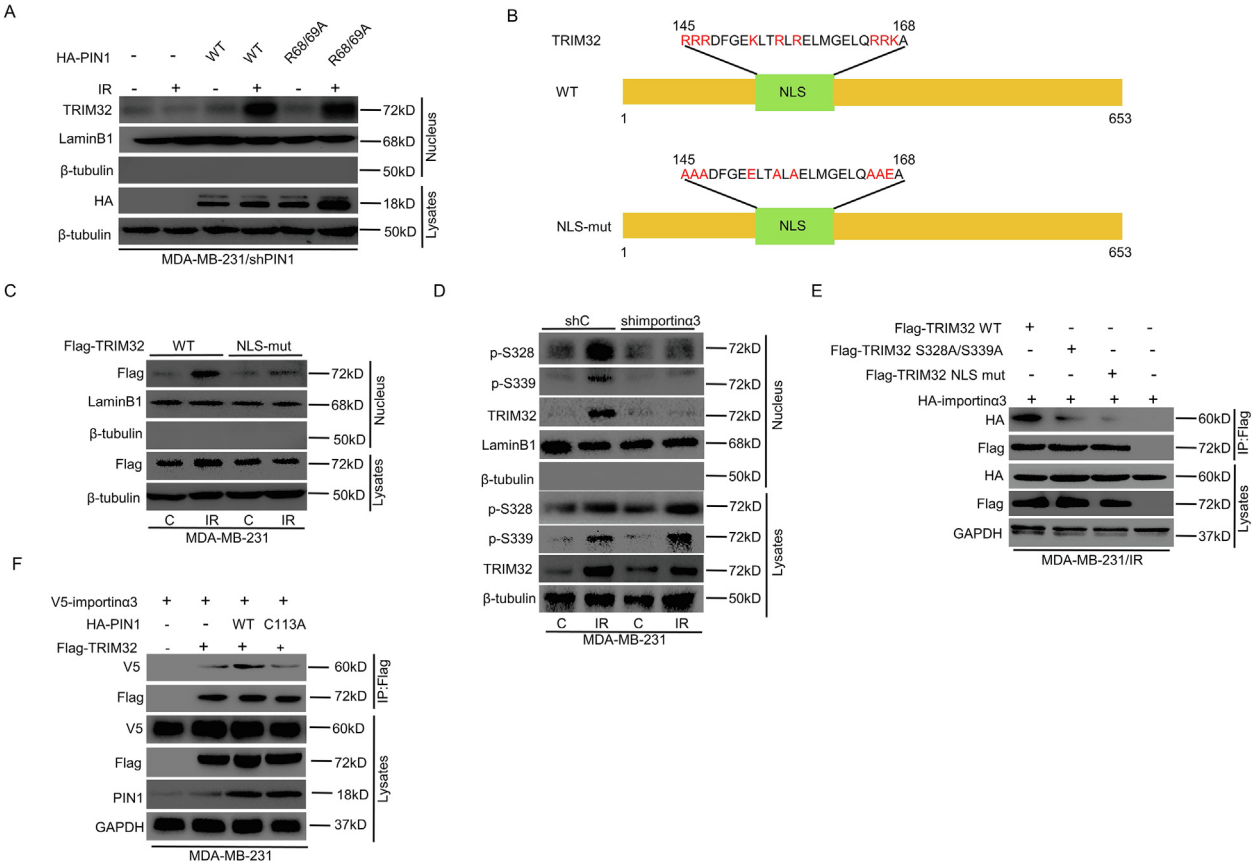

Fig. 4. PIN1 induces phosphorylated TRIM32 at S328 and S339 sites interacting with importin α3. A, Effect of re-expression of PIN1 WT and R68/69A mutant on TRIM32 nuclear translocation MDA-MB-231/shPIN1 cells. **B**, Schematics of TRIM32 WT and nuclear localization sequence (NLS) mutant. **C**, Representative images of effects of TRIM32 WT or NLS-mut on the nuclear translocation of TRIM32. **D**, WB assay for effects of importin α3 knockdown on the nuclear translocation of TRIM32 and phosphorylation of TRIM32 at S339 and S328 with or without radiotherapy. **E**, IP and WB assays for effects of TRIM32 WT, S328A/S339A, or NLS-mut on TRIM32 associated with importin α3. **F**, WB assay for effects of ectopic expression of PIN1 WT or C113A mutant on TRIM32 associated with importin α3. Data are representative of three independent experiments with similar results.

These results indicate that the nuclear translocation of TRIM32 depends on TRIM32's NLS domain.

Importin α transport protein was demonstrated to recognize and then link NLS sequences, regulating the nuclear transport process [25]. Flag-TRIM32 was overexpressed with HA-importin α1, α3, α4, α5, α6, or α7 in MDA-MB-231/irradiation cells. Importin α3, but not other importins, was associated with TRIM32, as indicated in Supplementary Fig. 4. Furthermore, importin α3 knockdown impaired radiotherapy-induced nuclear translocation of TRIM32 and phosphorylation of TRIM32 at S339 and S328 (Fig. 4D). Additionally, TRIM32 S328A, S339A, and NLS mutant, but not WT, decreased the combination of importin α3 and TRIM32 in MDA-MB-231/irradiation cells (Fig. 4E), revealing the essential role of importin α3 in PIN1-promoted nuclear translocation of phosphorylated TRIM32 at the S328 and S339 sites. Finally, V5-importin α3 and Flag-TRIM32 were overexpressed with HA-PIN1 WT or C113A mutant in MDA-MB-231 cells, revealing that PIN1 WT induced TRIM32 interaction with importin α3, whereas the PIN1 C113A mutant decreased their association (Fig. 4F). Collectively, these data suggest that PIN1-regulated cis–trans isomerization of phosphorylated TRIM32 at S328 and S339 sites exposes the NLS of TRIM32, then interacting with importin α3.

Nuclear TRIM32 promotes STAT3 phosphorylation

RNA sequencing analysis was performed in MDA-MB-231/irradiation cells treated with CDK2 inhibitor Roscovitine (Fig. 5A) to reveal the downstream mechanism in nuclear TRIM32-induced TNBC radioresistance. Analysis of the Kyoto Encyclopedia of Genes and Genomes (KEGG) shows that JAK-STAT3 pathway is one of the top five pathways (Fig. 5B). QRT-PCR and WB tests were carried out to verify RNA sequencing results. As shown in Fig. 5C and 5D, STAT3 target genes (SOCS3, c-FOS) [23] were down-regulated with Roscovitine in BT549/irradiated and MDA-MB-231/irradiation cells. Additionally, Roscovitine inhibited STAT3 phosphorylation but not STAT3 protein expression in MDA-MB-231/irradiation and BT549/irradiation cells (Fig. 5E). In conclusion, these results support that STAT3 signaling is regulated by CDK2 activity, and nuclear TRIM32 may mediate STAT3 signaling.

To demonstrate that nuclear TRIM32 promotes STAT3 phosphorylation, Flag-TRIM32 WT, S328A/S339A or NLS mutant were overexpressed in MDA-MB-231/irradiation/ shTRIM32 cells. Compared with the TRIM32 WT group, re-expression of shRNA-resistant TRIM32 S328A/S339A or NLS mutant impaired STAT3 phosphorylation, SOCS3 and c-FOS mRNA, cell proliferation and survival

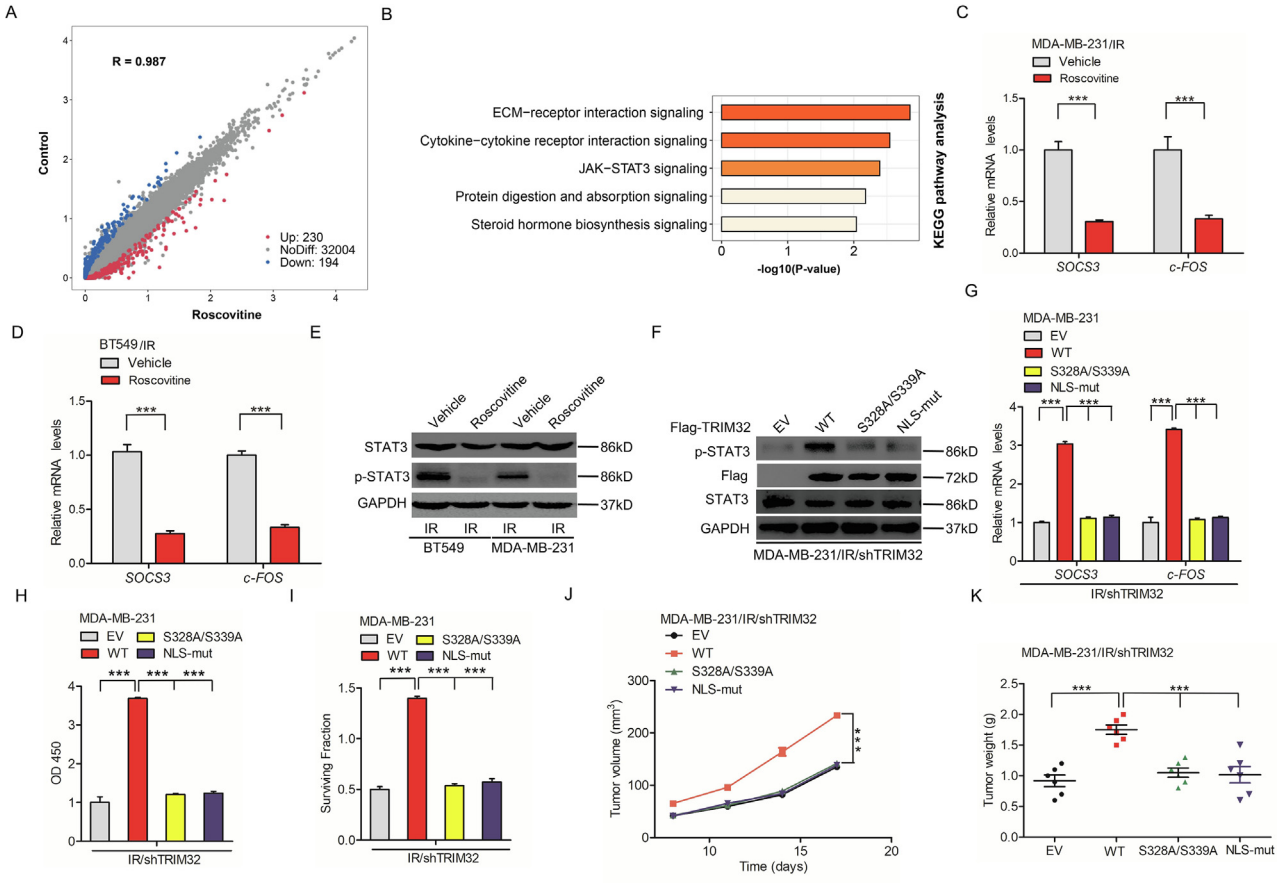

Fig. 5. Nuclear TRIM32 promotes STAT3 phosphorylation. A, Scatter plot of gene expression in MDA-MB-231/irradiation cells treated with (x-axis) or without (y-axis) Roscovitine (25 μM) for 1 h. Blue dots, set of genes significantly downregulated by Roscovitine; red dots, set of genes significantly upregulated by Roscovitine; gray dots, the genes without significant alteration. **B**, KEGG analysis revealed that the genes downregulated by the Roscovitine were predominantly associated with the JAK/STAT3 signaling pathway. **C-D**, Effects of Roscovitine on SOCS3 and c-FOS mRNA expression in MDA-MB-231/irradiation and BT549/ irradiation cells. **E**, WB assay for Roscovitine on STAT3 phosphorylation. **F**, Effects of TRIM32 WT, S328A/S339A, or NLS-mut on STAT3 phosphorylation in MDA-MB-231/ irradiation/shTRIM32 cells. **G-K**, Effects of re-expression of shRNA-resistant TRIM32 S328A/S339A or NLS mutant on SOCS3 and c-FOS mRNA (**G**), cell proliferation (**H**) and survival in vitro (**I**), tumor volume (**J**) and weight (**K**) in vivo in MDA-MB-231/ irradiation/shTRIM32 cells. Error bars ± S.D. ***P < 0.001. Data were representative of three independent experiments. (For interpretation of the references to colour in this figure legend, the reader is referred to the web version of this article.)

in vitro, as well as the tumor volume and weight in vivo (Fig. 5F to K). Interestingly, compared with the empty vector group, re-expression of TRIM32 WT resulted in an increase in the above items. Given the crucial roles of PIN1 and importin α3 in nuclear translocation of TRIM32, PIN1 and importin α3 were knocked down, respectively. Supplementary Fig. 5 suggests that PIN1 and importin α3 knockdown suppressed STAT3 phosphorylation, but not STAT3 protein expression in MDA-MB-231/irradiation cells. In conclusion, these data suggest that nuclear TRIM32 promotes STAT3 signaling, leading to enhanced TNBC radioresistance.

CDK2-activated TRIM32 phosphorylation disrupts STAT3-TC45 association

We recently demonstrated that TRIM32 promotes STAT3 phosphorylation and radioresistance in TNBC by disrupting TC45-STAT3 association [23]. Thus, we validated that nuclear TRIM32 promotes STAT3 signaling. Therefore, CDK2-activated TRIM32 phosphorylation may disrupt the STAT3-TC45 association. To test this hypothesis, IP and WB assays were performed. IP and WB assays revealed that STAT3 associated with TRIM32 in nucleus of MDA-MB-231/irradiation and BT549/irradiation-cells (Supplementally Fig. 7D). CDK2 inhibitor Roscovitine inhibited TRIM32-STAT3 interaction and STAT3 phosphorylation in MDA-MB-231/irradiation and BT549/irradiation cells (Fig. 6A). Moreover, Roscovitine induced TC45-STAT3 association (Fig. 6B), suggesting that CDK2-activated TRIM32 phosphorylation disrupts STAT3-TC45 association.

Consistent with our previous results [23], re-expression of TRIM32 WT increased TRIM32-STAT3 interaction and STAT3 phosphorylation by inhibiting STAT3-TC45 association compared with the empty vector group in MDA-MB-231/ irradiation/shTRIM32 cells (Fig. 6C and 6D). However, no change was found in the reexpression of non-phosphorylated TRIM32 S328A/S339A or NLS mutants (Fig. 6C and 6D). Furthermore, compared with the empty vector group, over-expression of PIN1 WT also enhanced TRIM32-STAT3 interaction and STAT3 phosphorylation by inhibiting STAT3-TC45 association in MDA-MB-231/irradiation cells, but PIN1 C113A overexpression did not show significant alteration on STAT3-TC45 interaction or STAT3 phosphorylation (Fig. 6E and 6F). Collectively, the results show that nuclear TRIM32-activated STAT3 signaling depends on suppressing TC45-dephosphorylated nuclear STAT3 to sustain high STAT3 phosphorylation.

Phosphorylation blockade of TRIM32 with CDK2 inhibitor Roscovitine inhibits tumorigenesis and radioresistance in TNBC in vitro and in vivo

To explore the treatment value of CDK2-phosphorylated TRIM32 blockade, the role of Roscovitine in TNBC proliferation was investigated in vitro, revealing that Roscovitine impedes TNBC cell proliferation and colony formation in vitro (Fig. 7A and 7B). Next, subcutaneous implantation of MDA-MB-231 cells into nude mice was performed, and Roscovitine was administered intraperitoneally. In line with the in vitro results, a 50 mg/kg concentration

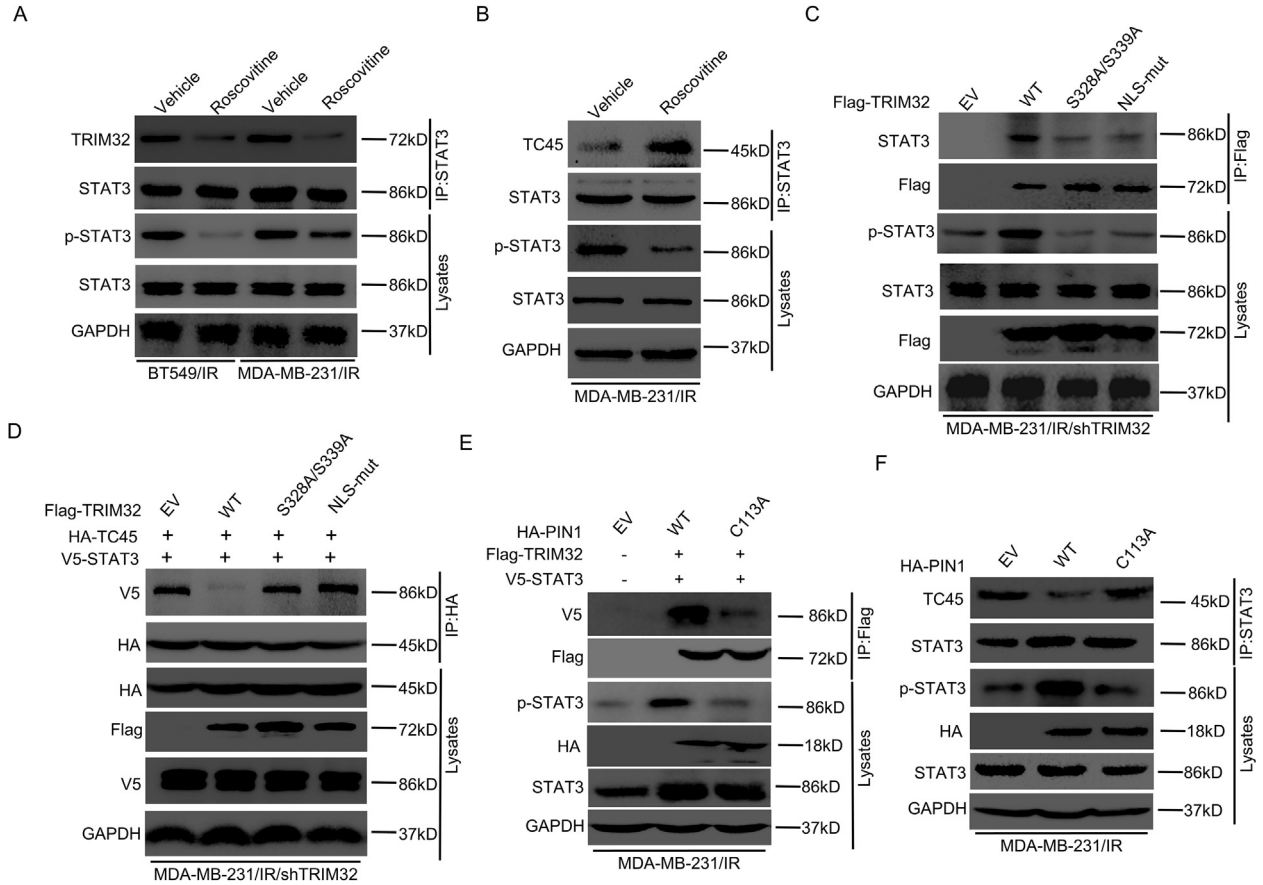

Fig. 6. CDK2-activated TRIM32 phosphorylation disrupts the STAT3-TC45 association. A, IP and WB assays for effects of Roscovitine on TRIM32 associated with STAT3. **B**, Effects of Roscovitine on STAT3 associated with TC45. **C**, IP and WB assays for effects of TRIM32 WT, S328A/S339A, or NLS-mut on TRIM32 binding with STAT3 in MDA-MB-231/irradiation/shTRIM32 cells. **D**, Representative images of effects of TRIM32 WT, S328A/S339A, or NLS-mut on TC45 associated with STAT3 in MDA-MB-231/irradiation/shTRIM32 cells. **E**, IP and WB assays for effects of PIN1 WT or C113A mutant on TRIM32 binding with STAT3 in MDA-MB-231/irradiation cells. **F**, Effects of PIN1 WT or C113A mutant on TC45 associated with STAT3 in MDA-MB-231/irradiation cells. Data are representative of three independent experiments with similar results.

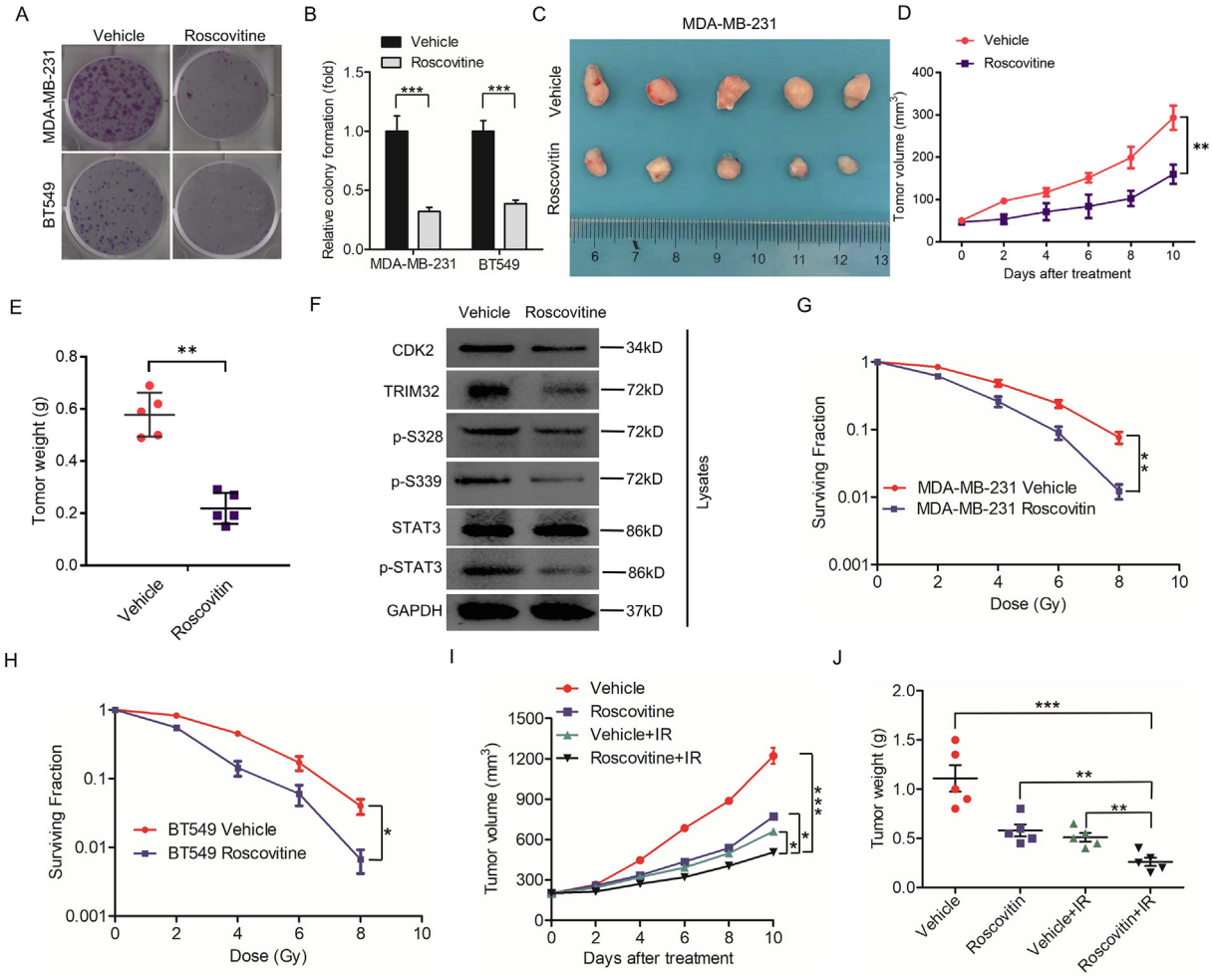

Fig. 7. Phosphorylation blockade of TRIM32 with CDK2 inhibitor Roscovitine inhibits tumorigenesis and radioresistance in TNBC in vitro and in vivo. A, Roscovitine impeded colony formation of MDA-MB-231 and BT549 cells. **B**, Quantitative analysis of colony numbers in **A**. **C-D**, The volume of the xenograft tumors in each group. Nude mice subcutaneously injected with MDA-MB-231 cells were treated with Roscovitine (Intraperitoneal injection, daily, 50 mg/kg concentration of Roscovitine) when the tumor volumes reached 150 mm^3 (n = five mice/group). **E**, The weight of the xenograft tumors in each group is shown (n = five mice/group). **F**, Western blot of the xenograft tumors extracted proteins. **G-H**, MDA-MB-231 and BT549 cells treated with Roscovitine at the indicated concentration for 24 h were irradiated at the indicated doses. The survival fraction was calculated after 2 weeks (n = 3). **I**, The volume of the xenograft tumors of each group. Nude mice were subcutaneously injected with MDA-MB-231 cells and treated with irradiation only, Roscovitine only or Roscovitine combination with 4 Gy irradiation (n = five mice/group). **J**, The weight of the xenograft tumors in each group (n = five mice/group). Data were presented as mean ± SEM. *P < 0.05, **P < 0.01. ***P < 0.001.

of Roscovitine led to significantly suppressed tumor volume and weight in vivo (Fig. 7C to 7E). The CDK2/TRIM32/STAT3 mechanism also operates in vivo (Fig. 7F). Therefore, these data indicated that phosphorylation blockade of TRIM32 with Roscovitine inhibits tumorigenesis of TNBC in vitro and in vivo.

Given nuclear TRIM32 induced the radioresistance of TNBC, a clonogenic survival assay was performed. As shown in Fig. 7G and H, Roscovitine significantly decreased radioresistance in MDA-MB-231 and BT549 cells. Moreover, the combination of irradiation and 50 mg/kg concentration of Roscovitine suppressed both tumor weight and volume more obviously compared with Roscovitine or irradiation treatment alone (Fig. 7I and J), suggesting that Roscovitine treatment effectively reduced TNBC radioresistance in vivo. In conclusion, these data supported that phosphorylation blockade of TRIM32 with CDK2 inhibitor Roscovitine inhibits radioresistance and tumorigenesis in TNBC in vitro and in vivo.

Clinical significance of CDK2/TRIM32/STAT3 pathway in TNBC

To further reveal the clinical significance of our data, a rabbit polyclonal antibody that specifically identifies p-TRIM32^{S339} and p-TRIM32^{S328} were generated, and its specificity for p-TRIM32^{S339} and p-TRIM32^{S328} in MDA-MB-231 cells and clinical TNBC tissues was tested (Supplementary Fig. 6). Subsequently, p-CDK2, p-TRIM32, and p-STAT3 were detected in 100 clinical TNBC samples. As shown in Fig. 8A, p-CDK2, p-TRIM32, and p-STAT3 were markedly co-expressed in TNBC specimens. Quantification of protein expression using IHC staining showed that the correlation was statistically significant (Fig. 8B). In addition, p-CDK2/p-TRIM32 and p-CDK2/p-STAT3 co-expression at high expression level are positively associated with poor prognosis in TNBC (Fig. 8C). These results indicate that the CDK2/TRIM32/STAT3 pathway showed a clinical prognosis value for TNBC.

Discussion

The findings reveal that CDK2 phosphorylated TRIM32 activates nuclear translocation, leading to enhanced STAT3 signaling activation and radioresistance in TNBC by suppressing TC45-dephosphorylated STAT3 (Fig. 8D). Radiotherapy is one of the major treatment strategies for decreasing TNBC recurrence and metastasis [30,31]. However, the mechanisms by which TNBC radioresistance occurs remain unclear. Nuclear translocation plays

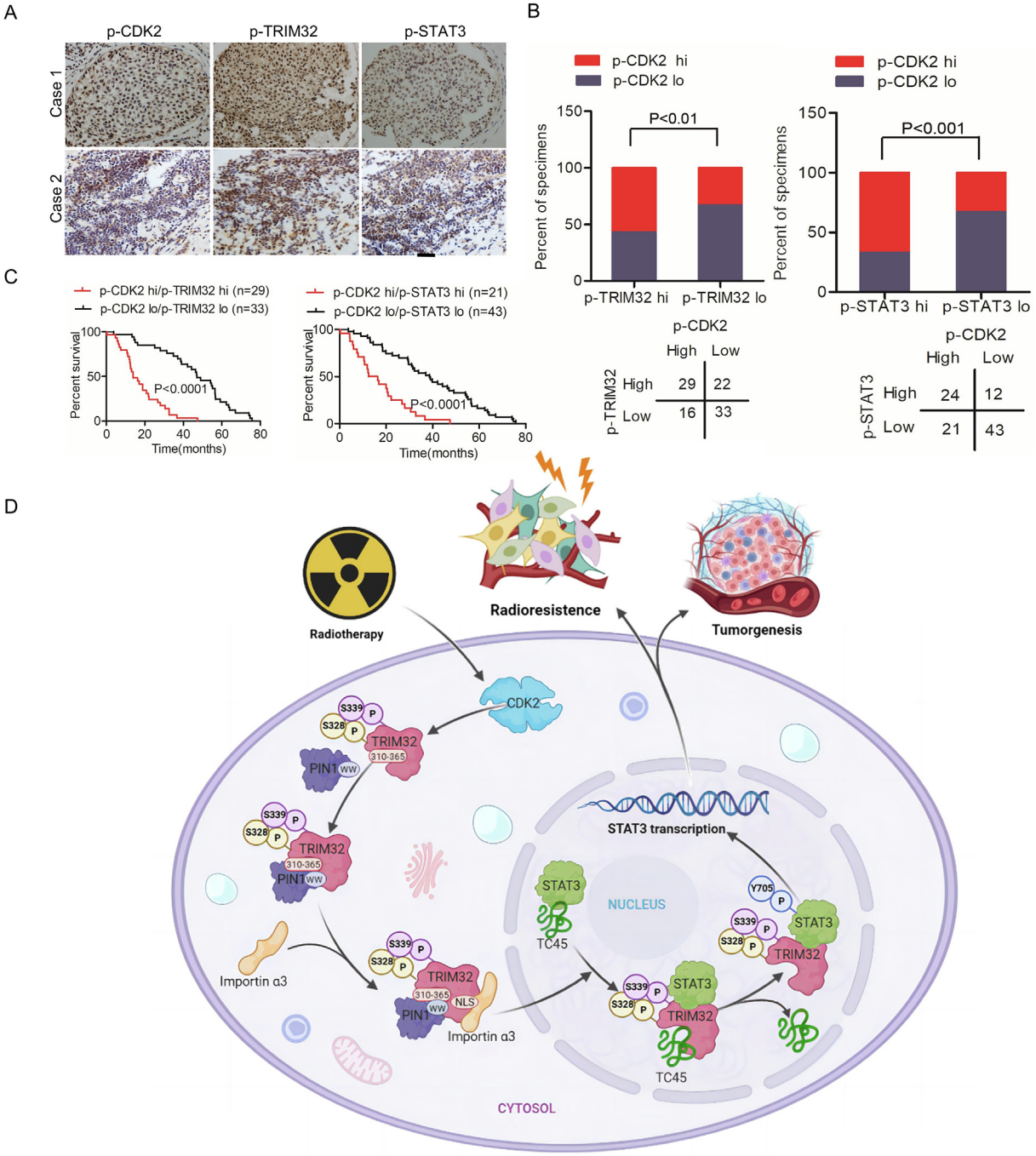

Fig. 8. Clinical significance of CDK2/TRIM32/STAT3 pathway in TNBC. A, Representative images of p-CDK2^{T14}, p-TRIM32^{S339}, and p-STAT3^{Y705} in 100 clinical TNBC tissues. Scale bars, 50 μm. **B**, Correlation of expression between p-CDK2^{T14}, p-TRIM32^{S339}, and p-STAT3^{Y705} in **A**. **C**, Kaplan-Meier comparison of patient prognosis with p-CDK2^{T14}/p-TRIM32^{S339} or p-CDK2^{T14}/p-STAT3^{Y705} differential expression. **D**, A working model of CDK2/TRIM32/STAT3 signaling in TNBC radioresistance.

a crucial role in radioresistance in TNBC [32,33]. EGFR nuclear translocation following irradiation was also reported to induce radiation resistance [34]. Our results supported the mechanism underlying nuclear translocation of TRIM32-driven TNBC radioresistance, which may enhance the curative effect of radiotherapy by inhibiting the newly identified CDK2/TRIM32 axis.

This data reveals that CDK2 induces TNBC radioresistance through TRIM32- promoted STAT3 signaling activation. CDK2 was reported to play a critical role in cancer initiation and progression [35–37]. CDK2-phosphorylated EZH2 at T416 promoted tumorsphere formation, cell migration and invasion as well as tumor growth in vivo [38]. CDK2 inhibitor effectively inhibits tumor growth and significantly prolongs the OS of mice carrying TNBC tumours [15]. Moreover, CDK2 improved the radiosensitivity of osteosarcoma [39]. In this investigation, we demonstrated that CDK2 induces radioresistance by promoting nuclear translocation of TRIM32 via the PIN1/importin α3 axis, thereby triggering enhanced STAT3 signaling in TNBC.

This study demonstrates that TRIM32 is a novel substrate of CDK2. Recent evidence supported that EZH2, and Smad3, have been demonstrated as substrates of CDK2 in TNBC [15,38,40]. TRIM32 was reported as an E3 ubiquitin ligase of ARID1A in

squamous cell carcinoma [41] and p53 in gastric cancer [21] and MYCN in human neuroblastoma [42]. In addition, TRIM32 functions as an oncogene in breast cancer [43], glioma [44],hepatocellular carcinoma [45] and gastric cancer [46]. We recently also reported that TRIM32 induces TNBC radioresistance by disrupting TC45-STAT3 interaction in TNBC [23]. In this study, TRIM32 was identified as a substrate of CDK2, which is phosphorylated at the S328 and S339 sites by CDK2 and is involved in nuclear translocation, thus leading to STAT3 signaling activation and radioresistance in TNBC. Furthermore, the combination of p-CDK2 with p-TRIM32 or p-STAT3 has a clinically prognostic significance in forecasting poor overall survival of TNBC.

This study also demonstrated that TRIM32 is directly associated with PIN1 or importin α3, resulting in its nuclear translocation. Nuclear translocation was reported to play critical roles in radioresistance of glioblastoma [47], prostate cancer [48], colorectal cancer [49],neuroblastoma [50],and lung cancer [51]. PIN1 regulates conformational alteration for p-Ser/Thr-Pro motifs and defines subsequent enzyme actions [25,26,52,53]. PIN1 has been confirmed to interact with phosphorylated PKM2 and cis–trans isomerized PKM2, inducing PKM2 translocation to the nucleus in glioblastoma [54]. Another study validated that MLK3 phosphorylated PIN1 on the S138 site, and the PIN1-pS138 translocated to the nucleus in pancreatic cancer [55]. Our research revealed that PIN1-mediated cis–trans isomerization of phosphorylated TRIM32 at S328 and S339 sites led to enhanced TRIM32 NLS exposure. Thus, PAK5 phosphorylated AIF at the Thr281 site and induced nuclear translocation of AIF by suppressing the formation of AIF/importin α3 complex, further promoting breast cancer tumorigenesis [56]. Nuclear localization sequence of RYBP, which includes Asn58 to Lys83, binds to importin α3 to allow nuclear translocation [57]. Our data further revealed that PIN1 induced phosphorylated TRIM32 at the S328 and S339 sites and interacted with importin α3, enhancing TRIM32 nuclear translocation. As a major regulating signaling pathway of radioresistance in cancer [58,59], STAT3 signaling has been linked to the nuclear translocation of key regulated genes in many cancers such as glioma [60], endometrial cancer [61], and breast cancer [62]. Our results identified nuclear TRIM32 promotes STAT3 signaling by suppressing TC45-dephosphorylated nuclear STAT3 to sustain high STAT3 phosphorylation.

In summary, we have identified a new mechanism by which CDK2 enhances STAT3 signaling activation and radioresistance through TRIM32 nuclear translocation. These results expand our understanding of the role of CDK2 in radioresistance to TNBC. Moreover, we provide new insights into the CDK2/TRIM32/STAT3 axis in radioresistance and therapeutic targets for preventing cancer radioresistance.

Acknowledgements

This study was supported, in part, by grants from the National Natural Science Foundation of China (Grant number: 82003236 to Haibo Zhang, 81972854 and 82272747 to Lei Zhang), Gansu Provincial National Science Foundation for Distinguished Young Scholars (Grant number: 21JR7RA389 to Jianming Tang), Medical Innovation and Development Project of Lanzhou University (Grant number: lzuyxcx-2022-162 to Jianming Tang), Fundamental Research Funds for the Central Universities (Grant number: lzujbky-2023-ey13 to Jianming Tang), National Innovation and Entrepreneurship Training Program for College Students (Grant number: 202210730171 to Yaqi Wang), Lanzhou University Undergraduate Innovation and Entrepreneurship Training Program (Grant number: 20220060218 to Zhitao Zhang), Zhejiang basic public welfare research plan project (Grant number: LY21H160051 to Min Fang).

Compliance with ethics requirements

This study was approved by Zhejiang Provincial People's Hospital's Research Ethics Board. All experiments were carried out in accordance with the protocol approved by Chinese Academy of Medical Science's Animal Care and Use Committee.

Declaration of Competing Interest

The authors declare that they have no known competing financial interests or personal relationships that could have appeared to influence the work reported in this paper.

Appendix A. Supplementary material

Supplementary data to this article can be found online at https://doi.org/10.1016/j.jare.2023.09.011.

References

[1] Lehmann BD, Bauer JA, Chen X, Sanders ME, Chakravarthy AB, Shyr Y, et al. Identification of human triple-negative breast cancer subtypes and preclinical models for selection of targeted therapies. J Clin Invest 2011;121(7):2750–67.
[2] Bonotto M, Gerratana L, Poletto E, Driol P, Giangreco M, Russo S, et al. Measures of outcome in metastatic breast cancer: insights from a real-world scenario. Oncologist 2014;19(6):608–15.
[3] He L, Lv Y, Song Y, Zhang B. The prognosis comparison of different molecular subtypes of breast tumors after radiotherapy and the intrinsic reasons for their distinct radiosensitivity. Cancer Manag Res 2019;11:5765–75.
[4] García-Aranda M, Redondo M. Protein Kinase Targets in Breast Cancer. Int J Mol Sci 2017;18(12):2543.
[5] Maemura M, Iino Y, Koibuchi Y, Yokoe T, Morishita Y. Mitogen-activated protein kinase cascade in breast cancer. Oncology 1999;57(Suppl 2):37–44.
[6] Sheng J, Zhao Q, Zhao J, Zhang W, Sun Y, Qin P, et al. SRSF1 modulates PTPMT1 alternative splicing to regulate lung cancer cell radioresistance. EBioMedicine 2018;38:113–26.
[7] Li M, Liu H, Zhao Q, Han S, Zhou L, Liu W, et al. Targeting Aurora B kinase with Tanshinone IIA suppresses tumor growth and overcomes radioresistance. Cell Death Dis 2021;12(2):152.
[8] Faber EB, Wang N, Georg GI. Review of rationale and progress toward targeting cyclin-dependent kinase 2 (CDK2) for male contraception†. Biol Reprod 2020;103(2):357–67.
[9] Fagundes R, Teixeira LK. Cyclin E/CDK2: DNA Replication, Replication Stress and Genomic Instability. Front Cell Dev Biol 2021;9:774845.
[10] Liu Q, Gao J, Zhao C, Guo Y, Wang S, Shen F, et al. To control or to be controlled? Dual roles of CDK2 in DNA damage and DNA damage response. DNA Repair (Amst) 2020;85:102702.
[11] Zardavas D, Pondé N, Tryfonidis K. CDK4/6 blockade in breast cancer: current experience and future perspectives. Expert Opin Invest Drugs 2017;26(12):1357–72.
[12] Tadesse S, Anshabo AT, Portman N, Lim E, Tilley W, Caldon CE, et al. Targeting CDK2 in cancer: challenges and opportunities for therapy. Drug Discov Today 2020;25(2):406–13.
[13] Jin X, Ge LP, Li DQ, Shao ZM, Di GH, Xu XE, et al. LncRNA TROJAN promotes proliferation and resistance to CDK4/6 inhibitor via CDK2 transcriptional activation in ER+ breast cancer. Mol Cancer 2020;19(1):87.
[14] Satriyo PB, Su CM, Ong JR, Huang WC, Fong IH, Lin CC, et al. 4-Acetylantroquinonol B induced DNA damage response signaling and apoptosis via suppressing CDK2/CDK4 expression in triple negative breast cancer cells. Toxicol Appl Pharmacol 2021;422:115493.
[15] Nie L, Wei Y, Zhang F, Hsu YH, Chan LC, Xia W, et al. CDK2-mediated site-specific phosphorylation of EZH2 drives and maintains triple-negative breast cancer. Nat Commun 2019;10(1):5114.
[16] Hatakeyama S. TRIM family proteins: roles in autophagy. Immun, carcinogenesisTrends Biochemical Sci 2017;42:297–311.
[17] Zhou Z, Ji Z, Wang Y, Li J, Cao H, Zhu HH, et al. TRIM59 Is up-regulated in gastric tumors, promoting ubiquitination and degradation of p53. Gastroenterology 2014;147:1043–54.
[18] Lazzari E, Meroni G. TRIM32 ubiquitin E3 ligase, one enzyme for several pathologies:from muscular dystrophy to tumours. Int J Biochem Cell Biol 2016;79:469–77.
[19] Wang C, Xu J, Fu H, Zhang Y, Zhang X, Yang D, et al. TRIM32 promotes cell proliferation and invasion by activating β-catenin signalling in gastric cancer. J Cell Mol Med 2018;22(10):5020–8.
[20] Wang M, Luo W, Zhang Y, Yang R, Li X, Guo Y, et al. Trim32 suppresses cerebellar development and tumorigenesis by degrading Gli1/sonic hedgehog signaling. Cell Death Differ 2020;27(4):1286–99.
[21] Liu J, Zhang C, Wang XL, Ly P, Belyi V, Xu-Monette ZY, et al. E3 ubiquitin ligase TRIM32 negatively regulates tumor suppressor p53 to promote tumorigenesis. Cell Death Differ 2014;21(11):1792–804.

[22] Wang J, Fang Y, Liu T. TRIM32 Promotes the Growth of Gastric Cancer Cells through Enhancing AKT Activity and Glucose Transportation. Biomed Res Int 2020;2020(11):4027627.
[23] Ma Y, Zhang H, Chen C, Liu L, Ding T, Wang Y, et al. TRIM32 promotes radioresistance by disrupting TC45-STAT3 interaction in triple-negative breast cancer. Oncogene 2022;41(11):1589–99.
[24] Zhu H, Nie L, Maki CG. Cdk2-dependent Inhibition of p21 stability via a C-terminal cyclin-binding motif. J Biol Chem 2005;280(32):29282–8.
[25] Zhou XZ, Lu KP. The isomerase PIN1 controls numerous cancer-driving pathways and is a unique drug target. Nat Rev Cancer 2016;16 (7):463–78.
[26] Yaffe MB, Schutkowski M, Shen M, Zhou XZ, Stukenberg PT, Rahfeld JU, et al. Sequence-specific and phosphorylation-dependent proline isomerization: a potential mitotic regulatory mechanism. Science 1997;278(5345):1957–60.
[27] Lufei C, Cao X. Nuclear import of Pin1 is mediated by a novel sequence in the PPIase domain. Nuclear import of Pin1 is mediated by a novel sequence in the PPIase domain. FEBS Lett 2009;583:271–6.
[28] Sang Y, Li Y, Zhang Y, Alvarez AA, Yu B, Zhang W, et al. CDK5-dependent phosphorylation and nuclear translocation of TRIM59 promotes macroH2A1 ubiquitination and tumorigenicity. Nat Commun 2019;10(1):4013.
[29] Nguyen Ba AN, Pogoutse A, Provart N, Moses AM. NLStradamus: a simple Hidden Markov Model for nuclear localization signal prediction. BMC Bioinf 2009;10:202.
[30] He MY, Rancoule C, Rehailia-Blanchard A, Espenel S, Trone JC, Bernichon E, et al. Radiotherapy in triple-negative breast cancer: Current situation and upcoming strategies. Crit Rev Oncol Hematol 2018;131:96–101.
[31] Burguin A, Diorio C, Durocher F. Breast Cancer Treatments: Updates and New Challenges. J Pers Med 2021;11(8):808.
[32] Qin S, He X, Lin H, Schulte BA, Zhao M, Tew KD, et al. Nrf2 inhibition sensitizes breast cancer stem cells to ionizing radiation via suppressing DNA repair. Free Radic Biol Med 2021;169:238–47.
[33] Ko H, Lee JH, Kim HS, Kim T, Han YT, Suh YG, et al. Novel Galiellalactone Analogues Can Target STAT3 Phosphorylation and Cause Apoptosis in Triple-Negative Breast Cancer. Biomolecules 2019;9(5):170.
[34] Zou M, Li Y, Xia S, Chu Q, Xiao X, Qiu H, et al. Knockdown of CAVEOLIN-1 Sensitizes Human Basal-Like Triple-Negative Breast Cancer Cells to Radiation. Cell Physiol Biochem 2017;44(2):778–91.
[35] Chohan TA, Qian H, Pan Y, Chen JZ. Cyclin-dependent kinase-2 as a target for cancer therapy: progress in the development of CDK2 inhibitors as anti-cancer agents. Curr Med Chem 2015;22(2):237–63.
[36] Tang Z, Li L, Tang Y, Xie D, Wu K, Wei W, et al. CDK2 positively regulates aerobic glycolysis by suppressing SIRT5 in gastric cancer. Cancer Sci 2018;109 (8):2590–8.
[37] Feng J, Wen T, Li Z, Feng L, Zhou L, Yang Z, et al. Cross-talk between the ER pathway and the lncRNA MAFG-AS1/miR-339-5p/ CDK2 axis promotes progression of ER+ breast cancer and confers tamoxifen resistance. Aging (Albany NY) 2020;12(20):20658–83.
[38] Yang CC, LaBaff A, Wei Y, Nie L, Xia W, Huo L, et al. Phosphorylation of EZH2 at T416 by CDK2 contributes to the malignancy of triple negative breast cancers. Am J Transl Res 2015;7(6):1009–20.
[39] Ran Q, Jin F, Xiang Y, Xiang L, Wang Q, Li F, et al. CRIF1 as a potential target to improve the radiosensitivity of osteosarcoma. PNAS 2019;116 (41):20511–6.
[40] Thomas AL, Lind H, Hong A, Dokic D, Oppat K, Rosenthal E, et al. Inhibition of CDK-mediated Smad3 phosphorylation reduces the Pin1-Smad3 interaction and aggressiveness of triple negative breast cancer cells. Cell Cycle 2017;16 (15):1453–64.
[41] Luo Q, Wu X, Nan Y, Chang W, Zhao P, Zhang Y, et al. TRIM32/USP11 Balances ARID1A Stability and the Oncogenic/Tumor-Suppressive Status of Squamous Cell Carcinoma. Cell Rep 2020;30(1):98–111.e5.
[42] Izumi H, Kaneko Y. Trim32 facilitates degradation of MYCN on spindle poles and induces asymmetric cell division in human neuroblastoma cells. Cancer Res 2014;74(19):5620–30.
[43] Zhao TT, Jin F, Li JG, Xu YY, Dong HT, Liu Q, et al. TRIM32 promotes proliferation and confers chemoresistance to breast cancer cells through activation of the NF-κB pathway. J Cancer 2018;9(8):1349–56.
[44] Cai Y, Gu WT, Cheng K, Jia PF, Li F, Wang M, et al. Knockdown of TRIM32 inhibits tumor growth and increases the therapeutic sensitivity to temozolomide in glioma in a p53-dependent and -independent manner. Biochem Biophys Res Commun 2021;550:134–41.
[45] Cui X, Lin Z, Chen Y, Mao X, Ni W, Liu J, et al. Upregulated TRIM32 correlates with enhanced cell proliferation and poor prognosis in hepatocellular carcinoma. Mol Cell Biochem 2016;421(1–2):127–37.
[46] Ito M, Migita K, Matsumoto S, Wakatsuki K, Tanaka T, Kunishige T, et al. Overexpression of E3 ubiquitin ligase tripartite motif 32 correlates with a poor prognosis in patients with gastric cancer. Oncol Lett 2017;13(5):3131–8.
[47] Zheng W, Chen Q, Liu H, Hu S, Zhou Y, Bai Y, et al. CD81 Enhances Radioresistance of Glioblastoma by Promoting Nuclear Translocation of Rad51. Cancers (Basel) 2021;13(9):1998.
[48] Luo Y, Li M, Zuo X, Basourakos SP, Zhang J, Zhao J, et al. β-catenin nuclear translocation induced by HIF-1α overexpression leads to the radioresistance of prostate cancer. Int J Oncol 2018;52(6):1827–40.
[49] Yang M, Liu Q, Dai M, Peng R, Li X, Zuo W, et al. FOXQ1-mediated SIRT1 upregulation enhances stemness and radio-resistance of colorectal cancer cells and restores intestinal microbiota function by promoting β-catenin nuclear translocation. J Exp Clin Cancer Res 2022;41(1):70.
[50] Aravindan S, Natarajan HTS, Aravindan N. Radiation-induced TNFα cross signaling-dependent nuclear import of NFκB favors metastasis in neuroblastoma. Clin Exp Metastasis 2013;30(6):807–17.
[51] Kim E, Youn H, Kwon T, Son B, Kang J, Yang HJ, et al. PAK1 tyrosine phosphorylation is required to induce epithelial-mesenchymal transition and radioresistance in lung cancer cells. Cancer Res 2014;74(19):5520–31.
[52] Zhou XZ, Kops O, Werner A, Lu PJ, Shen M, Stoller G, et al. Pin1-dependent prolyl isomerization regulates dephosphorylation of Cdc25C and tau proteins. Mol Cell 2000;6(4):873–83.
[53] Werner-Allen JW, Lee CJ, Liu P, Nicely NI, Wang S, Greenleaf AL, et al. cis-Proline-mediated Ser(P)5 dephosphorylation by the RNA polymerase II C-terminal domain phosphatase Ssu72. J Biol Chem 2011;286(7):5717–26.
[54] Yang W, Zheng Y, Xia Y, Ji H, Chen X, Guo F, et al. ERK1/2-dependent phosphorylation and nuclear translocation of PKM2 promotes the Warburg effect. Nat Cell Biol 2012;14(12):1295–304.
[55] Viswakarma N, Sondarva G, Principe DR, Nair RS, Kumar S, Singh SK, et al. Mixed Lineage Kinase 3 phosphorylates prolyl-isomerase PIN1 and potentiates GLI1 signaling in pancreatic cancer development. Cancer Lett 2021;515:1–13.
[56] Xing Y, Li Y, Hu B, Han F, Zhao X, Zhang H, et al. PAK5-mediated AIF phosphorylation inhibits its nuclear translocation and promotes breast cancer tumorigenesis. Int J Biol Sci 2021;17(5):1315–27.
[57] Neira JL, Jiménez-Alesanco A, Rizzuti B, Velazquez-Campoy A. The nuclear localization sequence of the epigenetic factor RYBP binds to human importin α3. Biochim Biophys Acta Proteins Proteom. 202;1869(8):140670.
[58] Wang X, Zhang X, Qiu C, Yang N. STAT3 contributes to radioresistance in cancer. Front Oncol 2020;10:1120.
[59] Park SY, Lee CJ, Choi JH, Kim JH, Kim JW, Kim JY, et al. The JAK2/STAT3/CCND2 Axis promotes colorectal Cancer stem cell persistence and radioresistance. J Exp Clin Cancer Res 2019;38:399.
[60] Zhang M, Sun H, Deng Y, Su M, Wei S, Wang P, et al. COPI-Mediated Nuclear Translocation of EGFRvIII Promotes STAT3 Phosphorylation and PKM2 Nuclear Localization. Int J Biol Sci 2019;15(1):114–26.
[61] Dai M, Yang B, Chen J, Liu F, Zhou Y, Zhou Y, et al. Nuclear-translocation of ACLY induced by obesity-related factors enhances pyrimidine metabolism through regulating histone acetylation in endometrial cancer. Cancer Lett 2021;513:36–49.
[62] Béguelin W, Díaz Flaqué MC, Proietti CJ, Cayrol F, Rivas MA, Tkach M, et al. Progesterone receptor induces ErbB-2 nuclear translocation to promote breast cancer growth via a novel transcriptional effect: ErbB-2 function as a coactivator of Stat3. Mol Cell Biol 2010;30(23):5456–72.
[63] Sang Y, Li Y, Song L, Alvarez AA, Zhang W, Lv D, et al. TRIM59 Promotes Gliomagenesis by Inhibiting TC45 Dephosphorylation of STAT3. Cancer Res 2018;78(7):1792–804.
[64] Yu B, Su J, Shi Q, Liu Q, Ma J, Ru G, et al. KMT5A-methylated SNIP1 promotes triple-negative breast cancer metastasis by activating YAP signaling. Nat Commun 2022;13(1):2192.